
Figures and figure supplements

Differential translation of mRNA isoforms underlies oncogenic activation of cell cycle kinase Aurora A

Roberta Cacioppo et al.

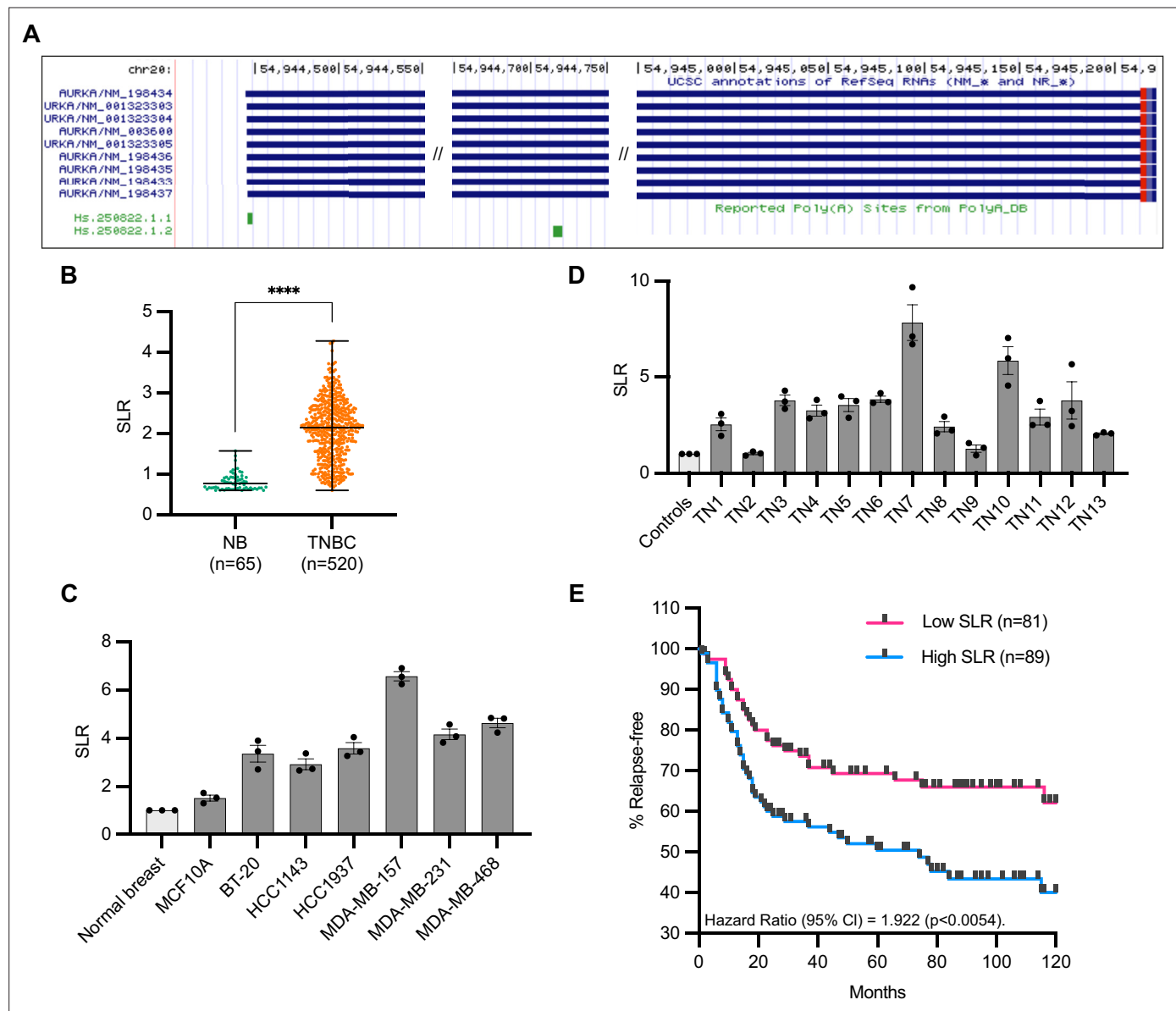


Figure 1. Increased short/long ratio (SLR) of Aurora Kinase A (AURKA) alternative polyadenylation (APA) isoforms in triple-negative breast cancer (TNBC). **(A)** AURKA transcript isoforms (USCS Genome Browser). AURKA gene is located on (-) strand. **(B)** Median and range of SLR values for AURKA 3'UTR obtained using APADetect. Mann–Whitney test; **** $p < 0.0001$. **(C), (D)** RT-qPCR analysis of SLR of AURKA 3'UTR in TNBC cell lines **(C)** and patient samples **(D)**. SDHA used as reference gene. TN, tissue number. **(E)** Relapse-free survival rates of TNBC patients with high (highest 25%) or low (lowest 25%) AURKA SLRs. p -value determined by log-rank test.

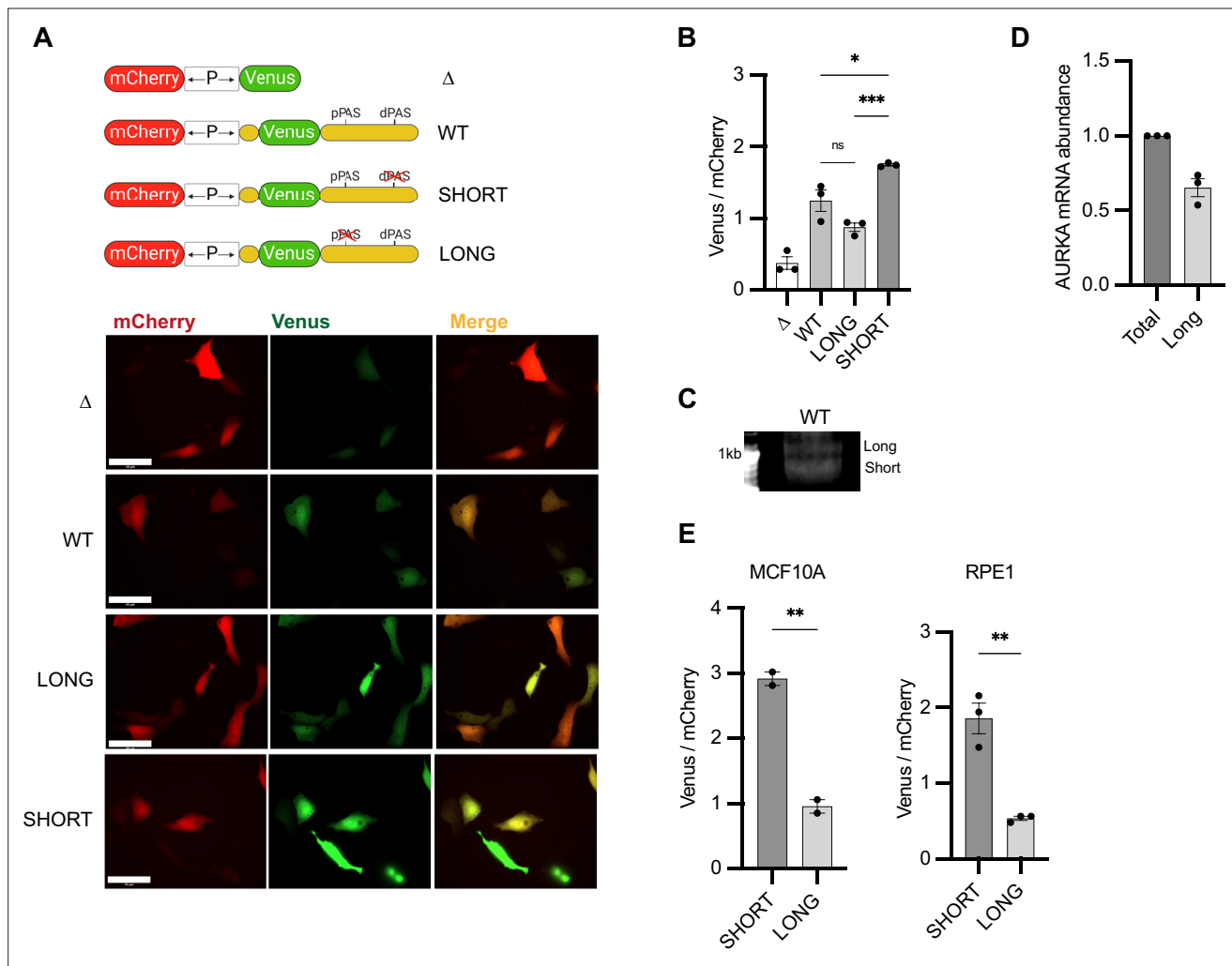


Figure 2. Aurora Kinase A (AURKA) shows 3'UTR isoform-dependent protein expression. **(A)** Top: UTR-dependent protein expression reporters. Venus coding sequence (CDS) is flanked by AURKA 5'UTR and 3'UTR, WT or polyadenylation signal (PAS)-mutated. Bottom: representative snapshots of transfected U2OS cells. Scale bar 50 μ m. **(B)** Mean and SEM of median Venus/mCherry mean fluorescence intensity (MFI) ratios from transfected U2OS cells from three biological replicates. $n \geq 129$ cells per condition. Ordinary one-way ANOVA with Tukeys multiple-comparisons test. **(C)** 3'RACE of endogenous AURKA APA isoforms. **(D)** RT-qPCR of endogenous AURKA short/long ratio (SLR) in U2OS cells. Long isoform abundance plotted as fold change over total AURKA mRNA. 18S rRNA used as reference target. **(E)** Same as **(B)** but in MCF10A (left) and RPE1 (right) cells. $n \geq 55$ cells per condition. Unpaired t-test. ns, not significant; *p<0.05; **p<0.01; ***p<0.001.

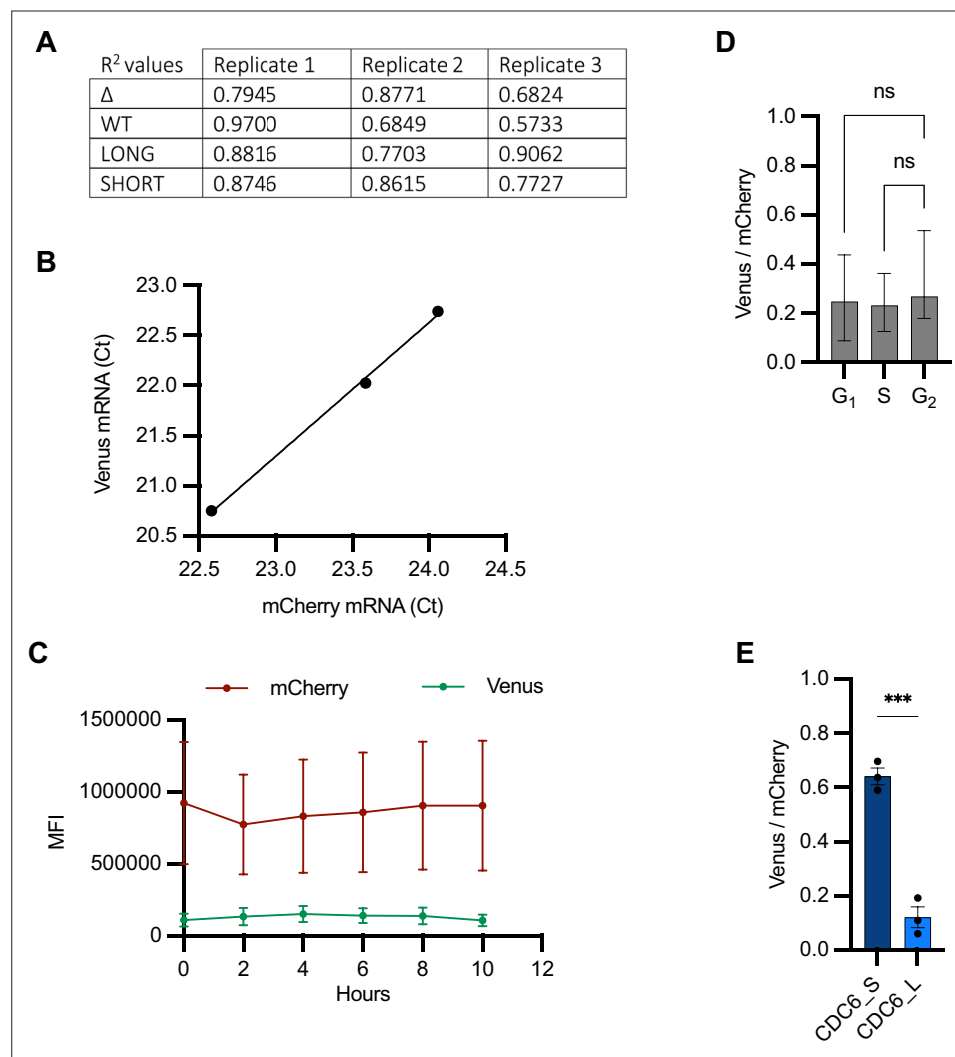


Figure 2—figure supplement 1. Validation of bidirectional reporter. **(A)** R² (coefficient of determination) values to indicate goodness of fit of a simple linear regression between mCherry and Venus single-cell mean fluorescence intensity (MFI) values. Data relative to **Figure 2B**. **(B)** RT-qPCR of mCherry and Venus mRNAs from three RNA extracts of U2OS cells transfected with Δ reporter. Ct values are mean between three technical replicates of the amplification reaction. **(C)** Quantification of mCherry and Venus MFI from U2OS cells transfected with the Δ reporter and imaged at the indicated time points. Mean and SEM (n = 8 cells) shown at each time point. **(D)** Single-cell Venus/mCherry MFI values from U2OS^{CDK2} cells transfected with Δ reporter grouped by intervals of CDK2 activity (**Figure 4A**, right) and plotted as median and 95% CI. n = 43 cells analyzed. Kruskal–Wallis with Dunnett’s multiple-comparisons test; ns, not significant. **(E)** Mean and SEM of median Venus/mCherry MFI ratios from U2OS cells transfected with constructs containing long or short CDC6 3’UTR from three biological replicates. n \geq 119 cells per condition. Unpaired t-test; ***p=0.0005.

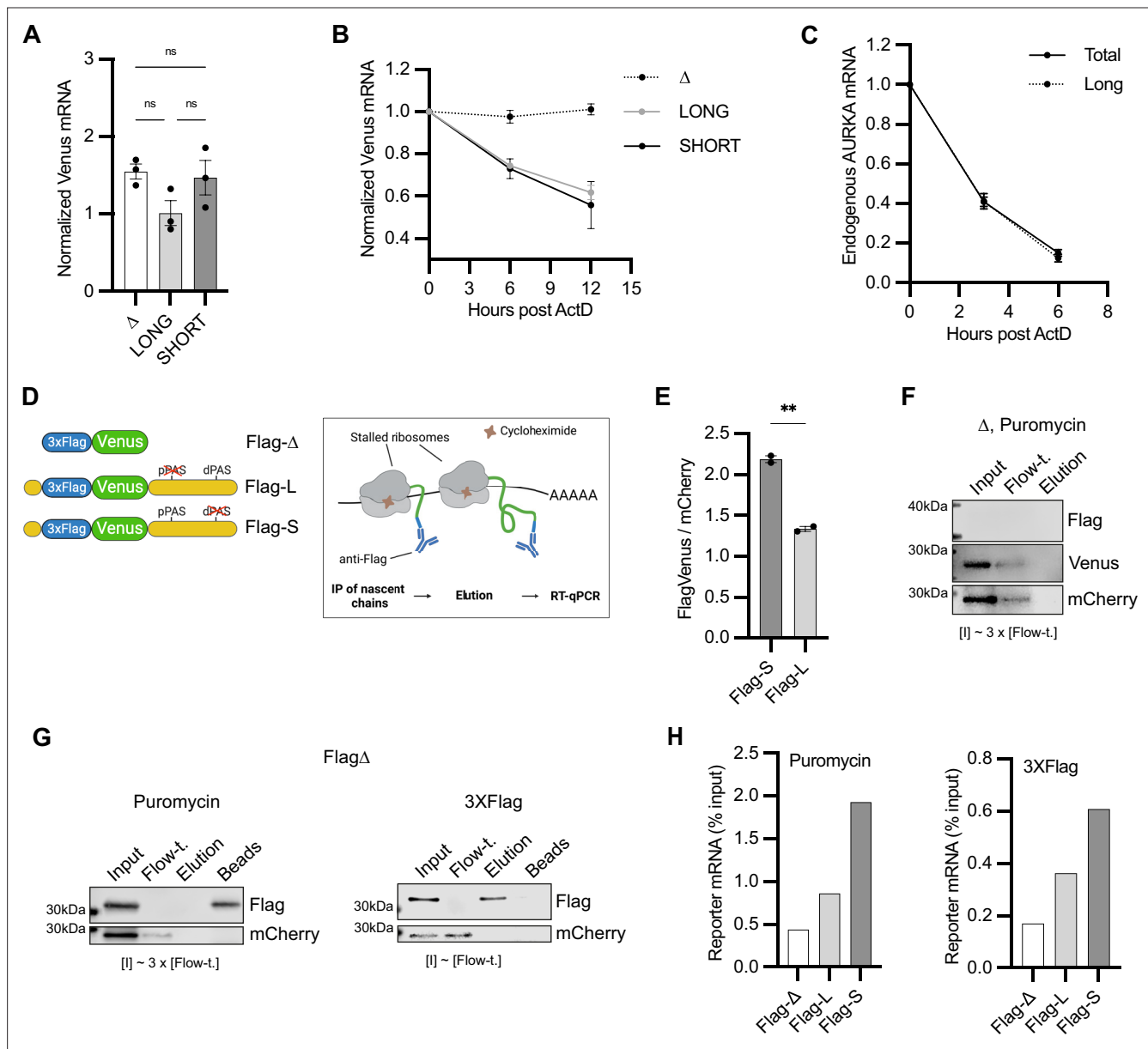
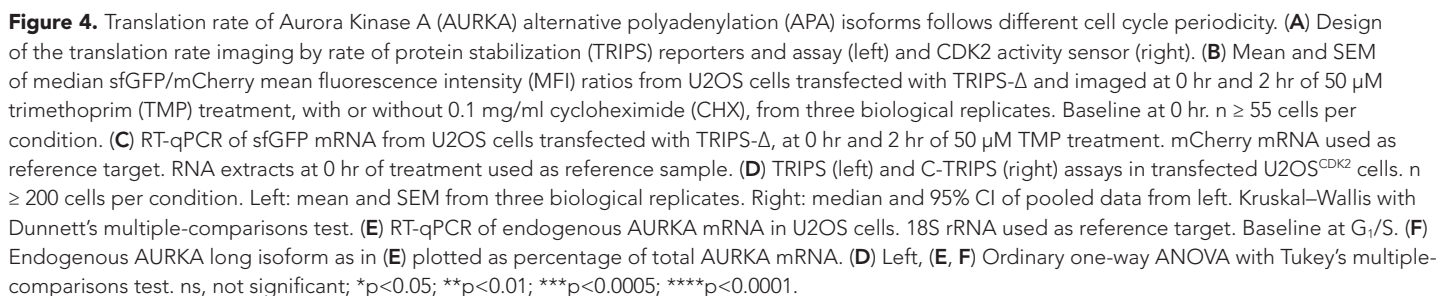


Figure 3. Aurora Kinase A (AURKA) alternative polyadenylation (APA) isoforms are translated with different efficiency. (**A**, **B**) RT-qPCR of reporter mRNAs abundance (**A**) and decay rate (**B**) from transfected U2OS cells. mCherry mRNA used as reference target. Ordinary one-way ANOVA with Tukey's multiple-comparisons test; ns, not significant. (**C**) Decay rate of endogenous AURKA mRNA as in (**B**). 18S rRNA used as reference target. Abundance of long isoform plotted as fold change over total AURKA mRNA. (**D**) Design of the nascent chain immunoprecipitation (NC IP) reporters and assay. (**E**) Mean and SEM of median FlagVenus/mCherry mean fluorescence intensity (MFI) ratios from transfected U2OS cells from two biological replicates. $n \geq 160$ cells per condition. Unpaired t-test; ** $p < 0.005$. (**F**), (**G**) Immunoblots of NC IP fractions using Δ (**F**) or Flag- Δ (**G**) reporter. mCherry used as negative control. (**H**) RT-qPCR of eluted reporter mRNAs. Results representative of three biological replicates.



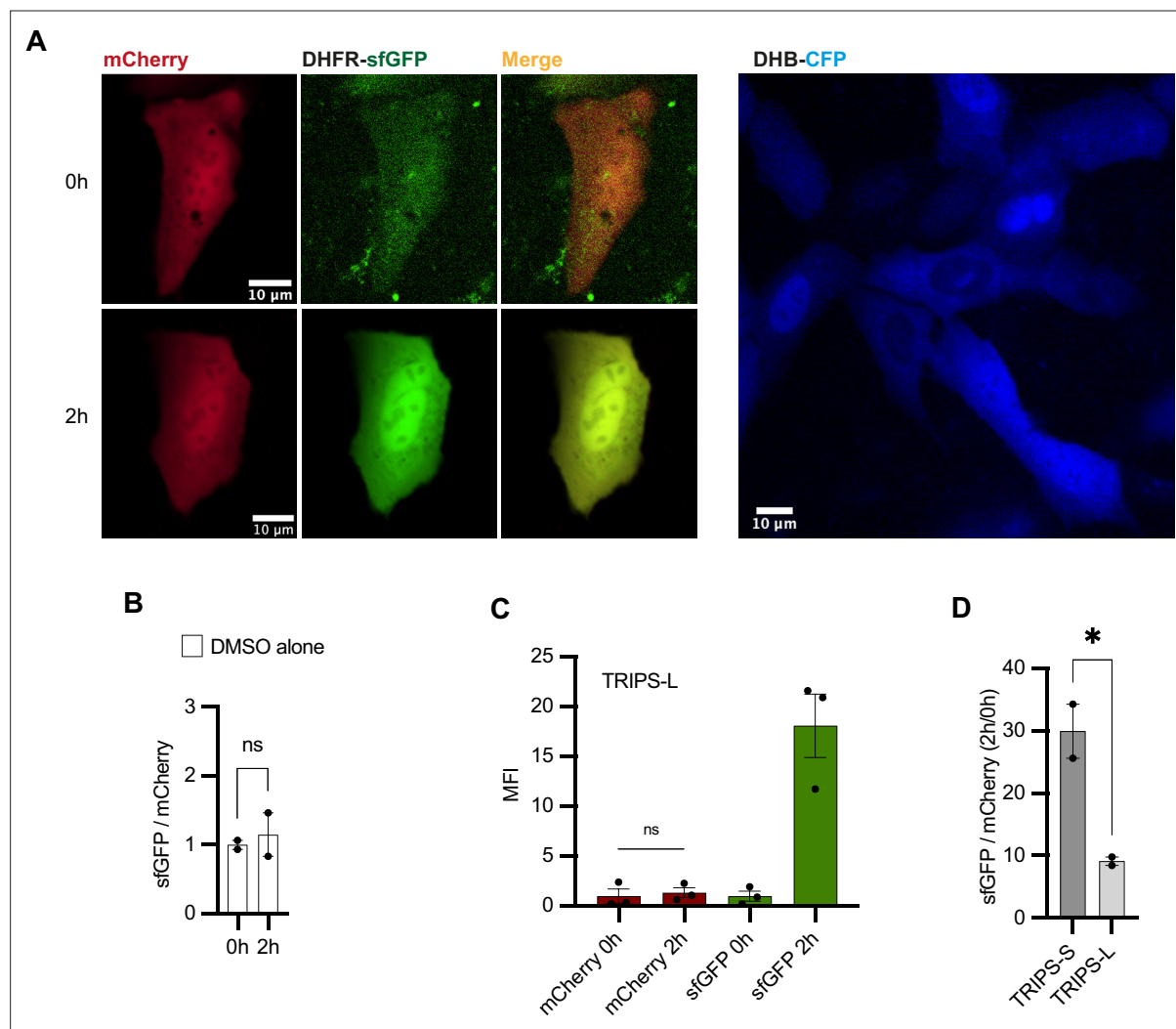


Figure 4—figure supplement 1. Validation of TRIPS assay. **(A)** Left: representative U2OS cells transfected with TRIPS-S and imaged at 0 hr and 2 hr of 50 μ M trimethoprim (TMP) treatment. Right: representative U2OS^{CDK2} cells. **(B)** TRIPS assay performed in U2OS cells transfected with TRIPS- Δ and treated with DMSO for 2 hr. Mean and SEM of median sfGFP/mCherry ratios from two biological replicates, with baseline at 0 hr. $n = 95$ cells analyzed. **(C)** Graph using data from **Figure 4D** showing mean fluorescence intensity (MFI) of mCherry and sfGFP at 0 hr and 2 hr of TMP treatment. Mean and SEM of median MFI values from three biological replicates. **(D)** TRIPS assay performed in transfected U2OS cells and imaged at 0 hr and 2 hr of 50 μ M TMP treatment. Ratios between the median of single-cell sfGFP/mCherry ratios at 2 hr and that at 0 hr of TMP treatment were calculated for two biological replicates and are shown as mean and s.e.mSEM. $n \geq 343$ cells analyzed per condition. **(B–D)** Unpaired t -test. ns, not significant; * $p < 0.05$.

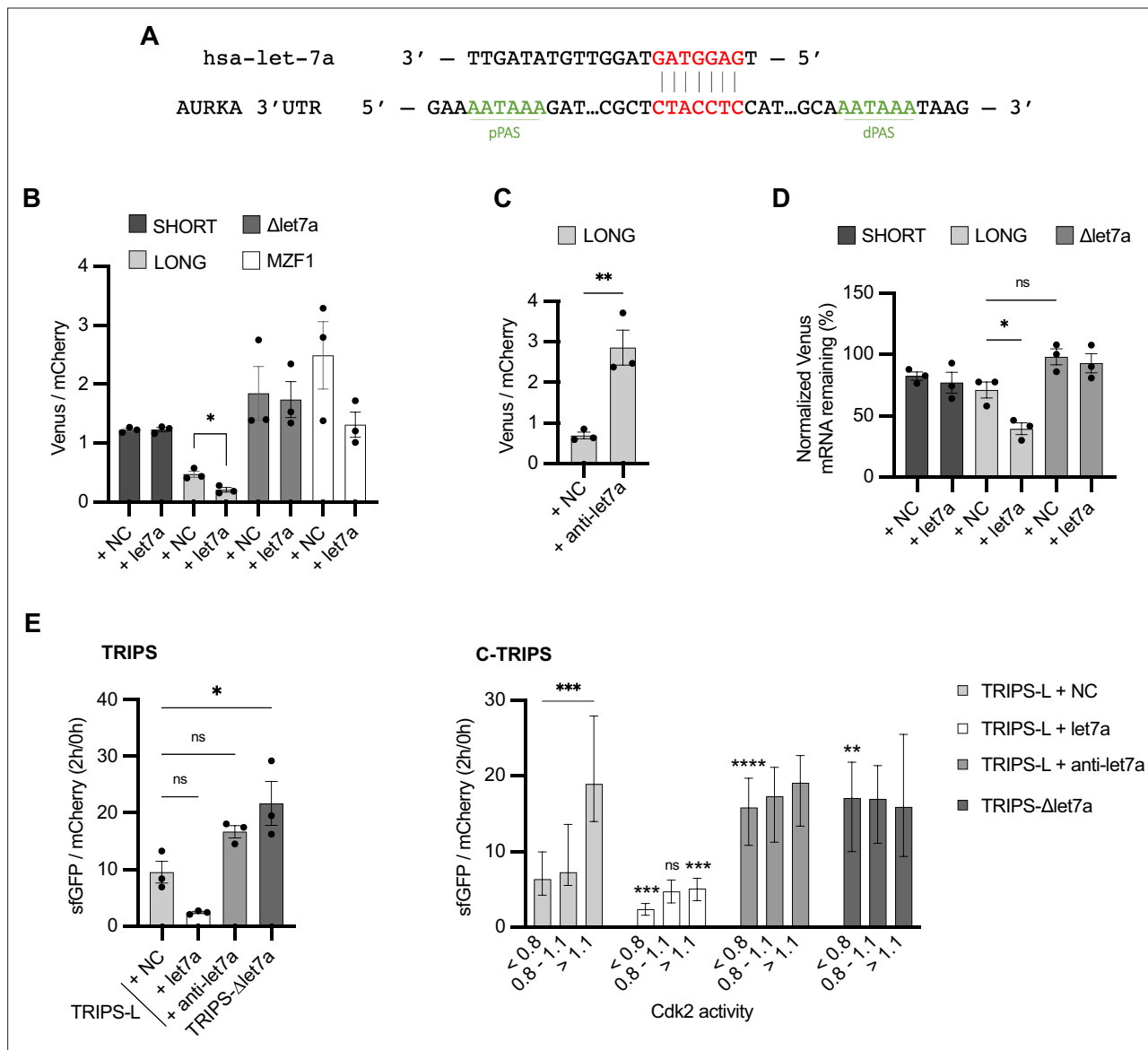


Figure 5. Translational periodicity of long 3'UTR isoform is regulated by *hsa-let-7a* miRNA. **(A)** Complementarity of *hsa-let-7a* binding to Aurora Kinase A (AURKA) 3'UTR. **(B)** Mean and SEM of median Venus/mCherry mean fluorescence intensity (MFI) ratios from U2OS cells co-transfected with 250 nM *hsa-let-7a* or a negative control (NC) miRNA from three biological replicates. $n \geq 182$ cells per condition. Unpaired *t*-test. **(C)** Same as **(B)** but co-transfecting 300 nM *anti-let-7a* or NC. $n \geq 94$ cells per condition. Unpaired *t*-test. **(D)** RT-qPCR of reporter mRNAs abundance from U2OS cells transfected as **(B)**, at 8 hr of 10 μ g/ml ActD. mCherry mRNA used as reference target. Ordinary one-way ANOVA with Tukey's multiple-comparisons test. **(E)** Translation rate imaging by rate of protein stabilization (TRIPS) (left) and C-TRIPS (right) assays in transfected U2OS^{CDK2} cells. $n \geq 162$ cells per condition. Left: mean and SEM from three biological replicates. Ordinary one-way ANOVA with Dunnett's multiple-comparisons test vs. NC. Right: median and 95% CI of pooled data from left. Kruskal-Wallis with Dunnett's multiple-comparisons test vs. NC of the respective phase. ns, not significant; * $p < 0.05$; ** $p < 0.01$; *** $p < 0.001$; **** $p < 0.0001$.

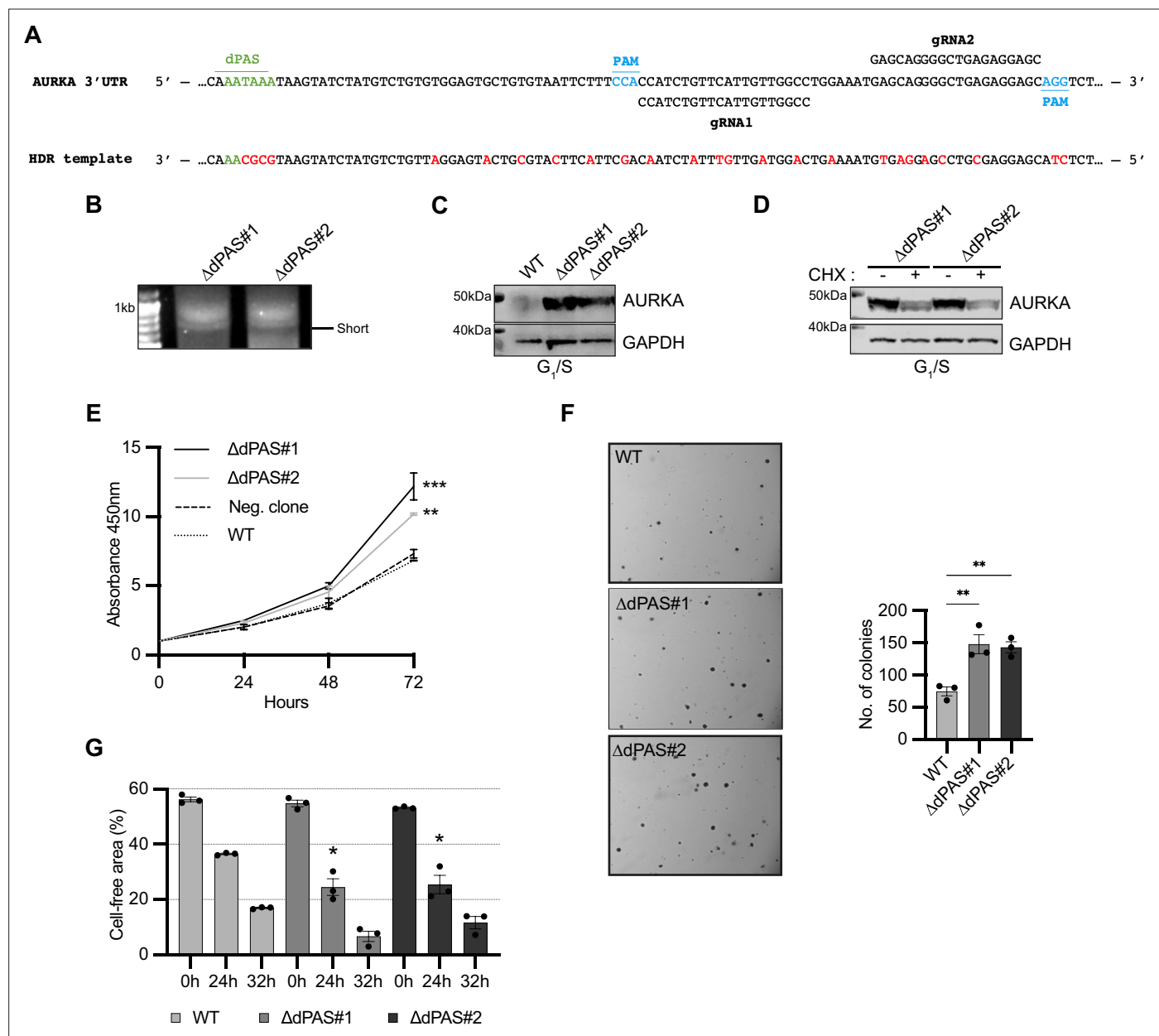


Figure 6. Increased Aurora Kinase A (AURKA) short/long ratio is sufficient to disrupt cell behavior. **(A)** Design of CRISPR editing. Nucleotide substitutions in red. **(B)** 3'RACE of endogenous AURKA alternative polyadenylation (APA) isoforms. **(C), (D)** Western blot after G₁/S enrichment **(C)** and with or without 6 hr treatment with 0.1 mg/ml cycloheximide (CHX) **(D)**. Blots representative of three biological replicates. **(E)** CCK8 assay. A nonparental WT U2OS cell line used as negative control. Ordinary one-way ANOVA with Dunnett's multiple-comparisons test vs. WT; **p<0.005; ***p<0.001. **(F)** Left: representative images of cells grown in soft agar. Right: mean number of clones and SEM of three biological replicates. **(G)** Measurement of migration rate. **(F, G)** Ordinary one-way ANOVA with Dunnett's multiple-comparisons test vs. WT; *p<0.05; **p<0.01.

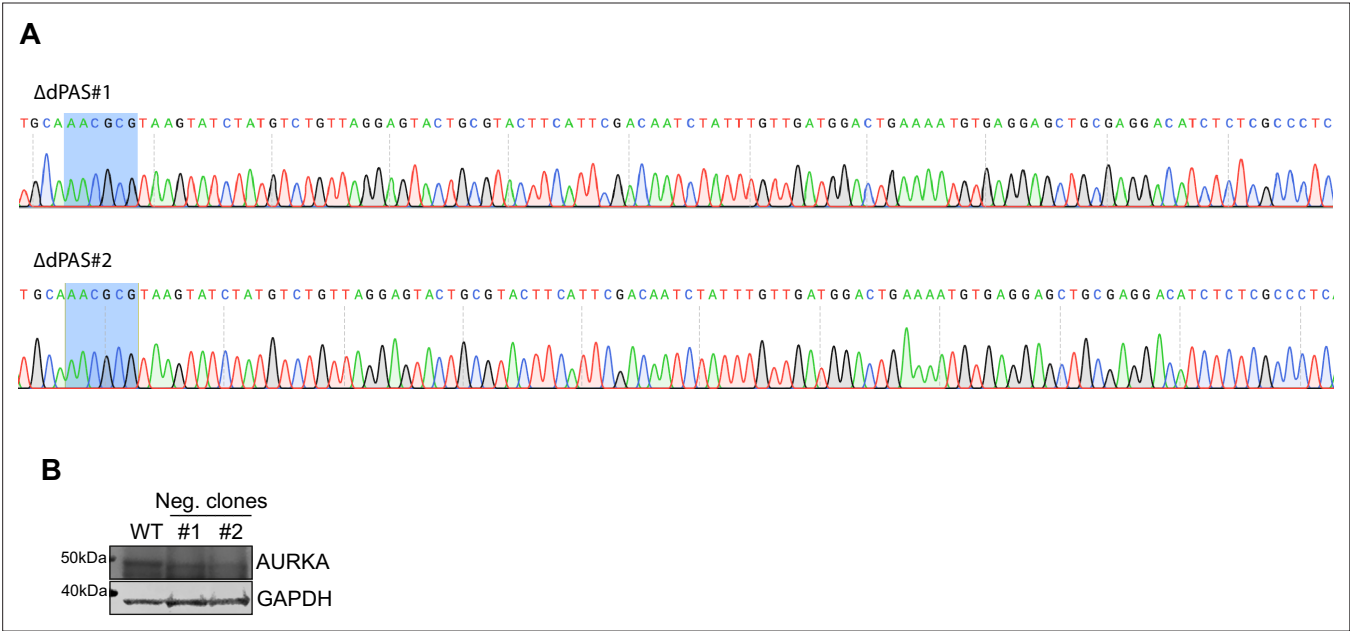
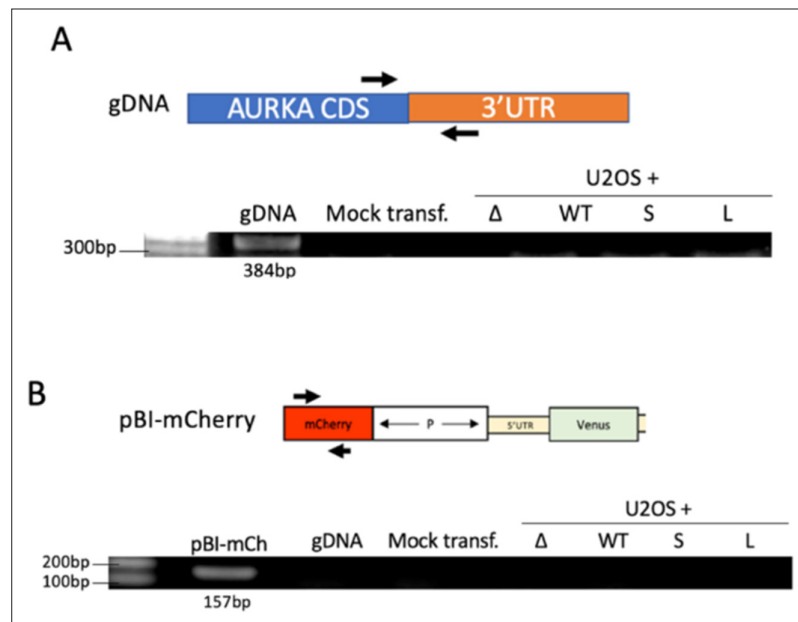


Figure 6—figure supplement 1. Validation of mutated cell lines. **(A)** Sanger sequencing validation of the mutated dPAS element in two cell lines. **(B)** Western blot showing similar Aurora Kinase A (AURKA) protein expression in unsynchronized WT or U2OS cell lines that were not mutated following CRISPR editing (#1, #2).



Appendix 1—figure 1. Assessment of DNA contamination of RNA extracts. **(A)** Lack of genomic DNA (gDNA) contamination in RNA samples was assessed by PCR using Aurora Kinase A (AURKA)-specific primers. RNA extracts from U2OS cells electroporated with the indicated reporters (**Figure 2A**) were used as template for the amplification reaction. An RNA extract from mock transfected U2OS cells used as negative control. gDNA from untransfected U2OS cells used as positive control. **(B)** Lack of plasmid DNA contamination in RNA samples was assessed by PCR using mCherry specific primers. RNA extracts from U2OS cells electroporated with the indicated reporters (**Figure 2A**) were used as template for the amplification reaction. An RNA extract from mock transfected U2OS cells and gDNA from untransfected U2OS cells used as negative controls. pBI-mCherry plasmid (pBI-mCh) used as positive control template.

UCSC In-Silico PCR

mCherry_F
mCherry_R

No matches to ccgacatccccgactactgaagc cacctttagatgaactcgccgtcc in Human Dec. 2013 (GRCh38/hg38)

3'UTR_F
3'UTR_R

No matches to gcccgacaaccactacctgagctac gctcaaggatttctccccctgcac in Human Dec. 2013 (GRCh38/hg38)

Venus_F
Venus_R

No matches to ctgacctgaagctgatct gcatggcggactgaagaag in Human Dec. 2013 (GRCh38/hg38)

18S_F
18S_R

RefSeq: [NR_146146.1](#) Status: Validated
Description: RNA, 18S ribosomal RNA N2
Molecule type: rRNA
>[chr21:8438122+8438231](#) 110bp CTCAACACGGGAAACCTCAC CGCTCCACCACTAAGAACG
CTCAACACGGGAAACCTCACccggcccgacacggacaggattgacagat
ttagtagctctttctcgattccgtgggtggtggtgcatggcCGTTCTTAGT
TGGTGGAGCG

sfGFP_F
sfGFP_R

No matches to ggccctgtcctttaccagacaacc catcatgccatgtgtaatcccagc in Human Dec. 2013 (GRCh38/hg38)

AURKA_Total_F
AURKA_Total_R

>[chr20:56370206-56370317](#) 112bp TGTAAACAGAGGGAGCCAGGGACC TGATGAATTTGCTGTGATCCAGGGGTG
TGTAAACAGAGGGAGCCAGGGACCTcatttcaagactgttgaagcataatc
ccagccagaggccaatgctcagagaagtacttgaacACCCCTGGATCACA
GCAAATTCATCA

AURKA_Long_F
AURKA_Long_R

>[chr20:56369488-56369738](#) 251bp GGCGAAGCCTGGTAAAGCTG GCCTCTTCTGTATCCCAAGCAAATCC
GGCGAAGCCTGGTAAAGCTGttggaatgagtatgtgattcttttaagta
tgaaataaagatatgtacagactgtatttttctctggtggcattc
cttaggaatgctgtgtgtctgtccggcaccgccgtaggcctgattgggt
tttagtctctccttaaccattatctcccatatgagagtgtgaaaaatag
gaacacgtgctctacctcatttagGGATTGCTTGGGATACAGAAGAGG
C

AURKA_SLR_F
AURKA_SLR_Short_R

>[chr20:56369717-56369878](#) 162bp TGCTAGGCATGGTGTCTTCA AACAGCTTTACCAGGCTTCG
TGCTAGGCATGGTGTCTTCAcaggaggcaaatccagagcctggctgtggg
gaaagtgaccactctgccctgacccgatcagtttaaggagctgtgcaata
accttcctagtacctgagtgagtggttaacttattgggttggCGAAGCCT
GGTAAAGCTGT

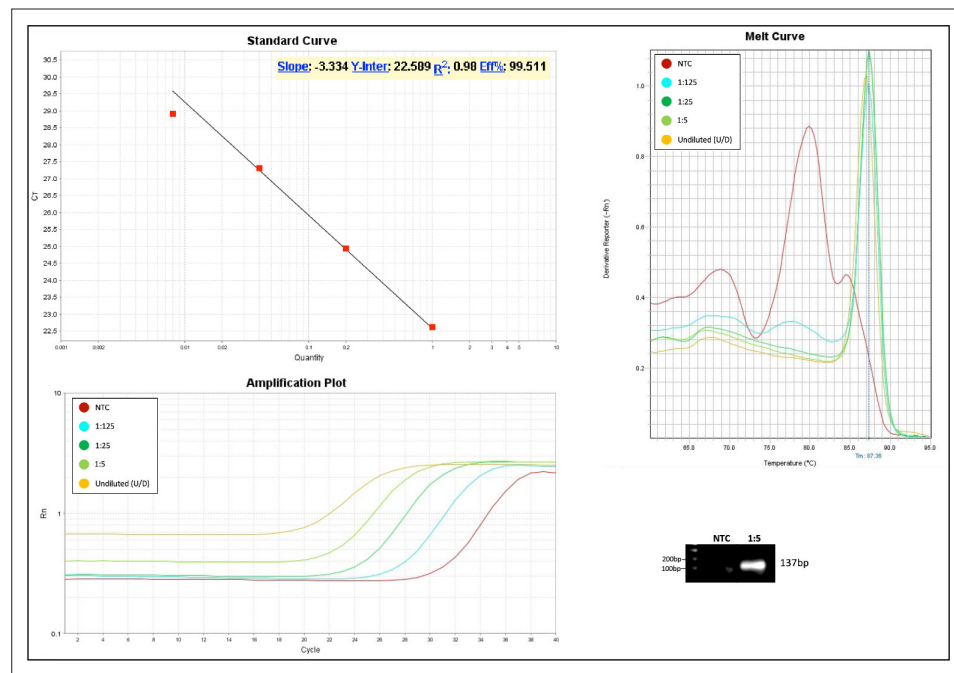
AURKA_SLR_F
AURKA_SLR_Long_R

>[chr20:56369585-56369878](#) 294bp TGCTAGGCATGGTGTCTTCA AGAAACCAATCAGGCCTAC
TGCTAGGCATGGTGTCTTCAcaggaggcaaatccagagcctggctgtggg
gaaagtgaccactctgccctgacccgatcagtttaaggagctgtgcaata
accttcctagtacctgagtgagtggttaacttattgggttggcgaagcct
ggtaaagctgttgggaatgagtatgtgattcttttaagtatgaaaataaa
gatatagtacagacttgatttttctctggtggcattccttttaggaat
gctgtgtgtctgtccggcaccgccGTAAGCCTGATTGGGTTCT

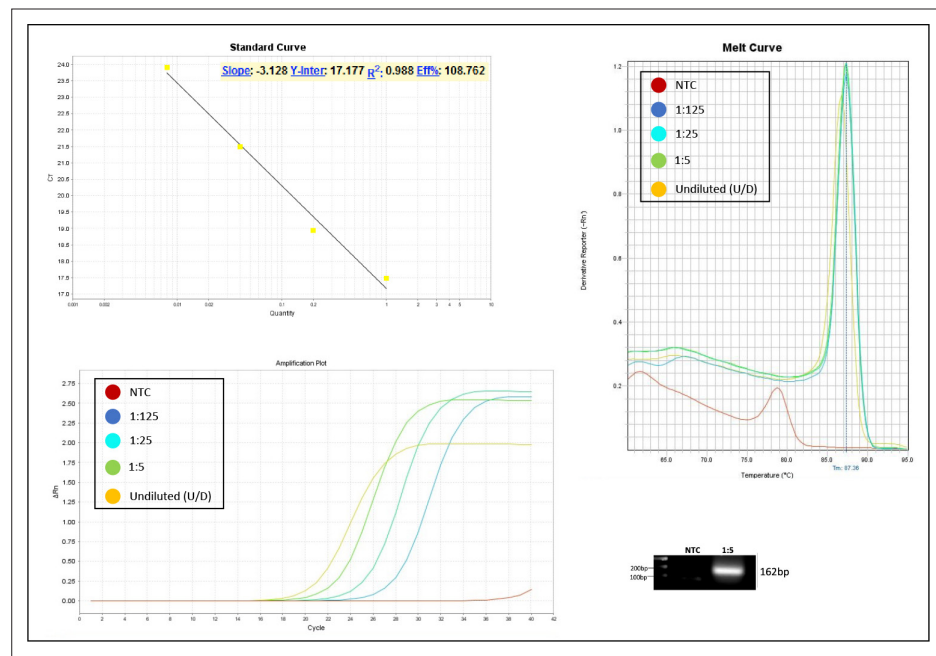
SDHA_F
SDHA_R

No matches to tgggaacaagagggcatctg ccaccactgcataaattca in Human Dec. 2013 (GRCh38/hg38)

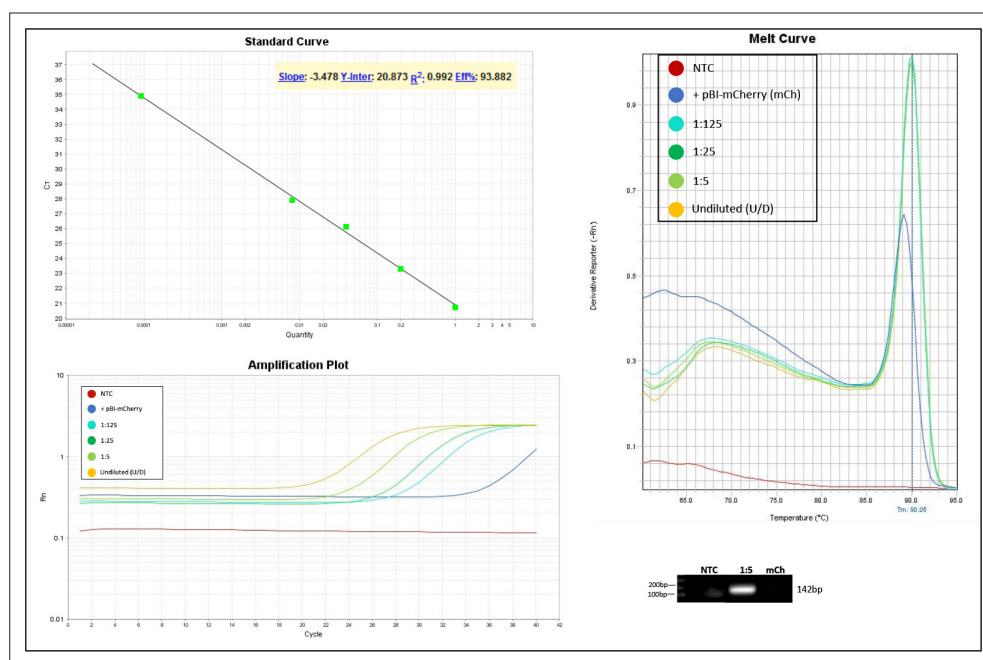
Appendix 1—figure 2. Predicted targets on human genome of primer pairs used in this study. Analysis performed using UCSC In-Silico PCR tool (<https://genome.ucsc.edu/cgi-bin/hgPcr>). Genomic PCR product of SDHA primer pairs is above >850 bp length set for the in silico search.



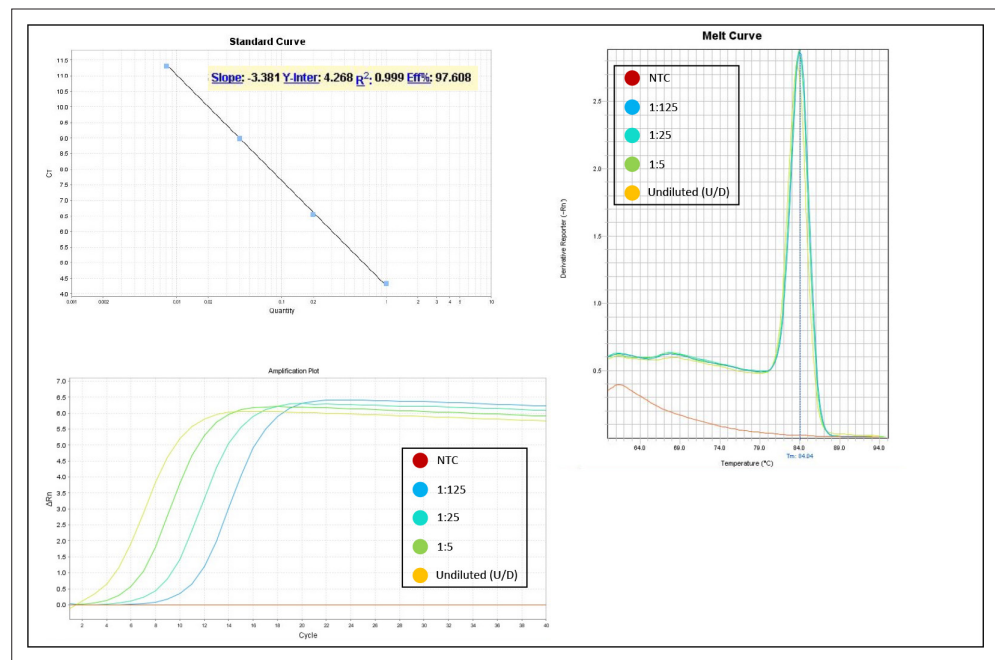
Appendix 1—figure 3. Validation of primer pairs used in RT-qPCR. Standard curve, melt curve, and amplification plot of amplification reactions of serial dilutions (1:5) are shown. Sample reactions were loaded on gel to validate amplicon size. NTC, non-template control.



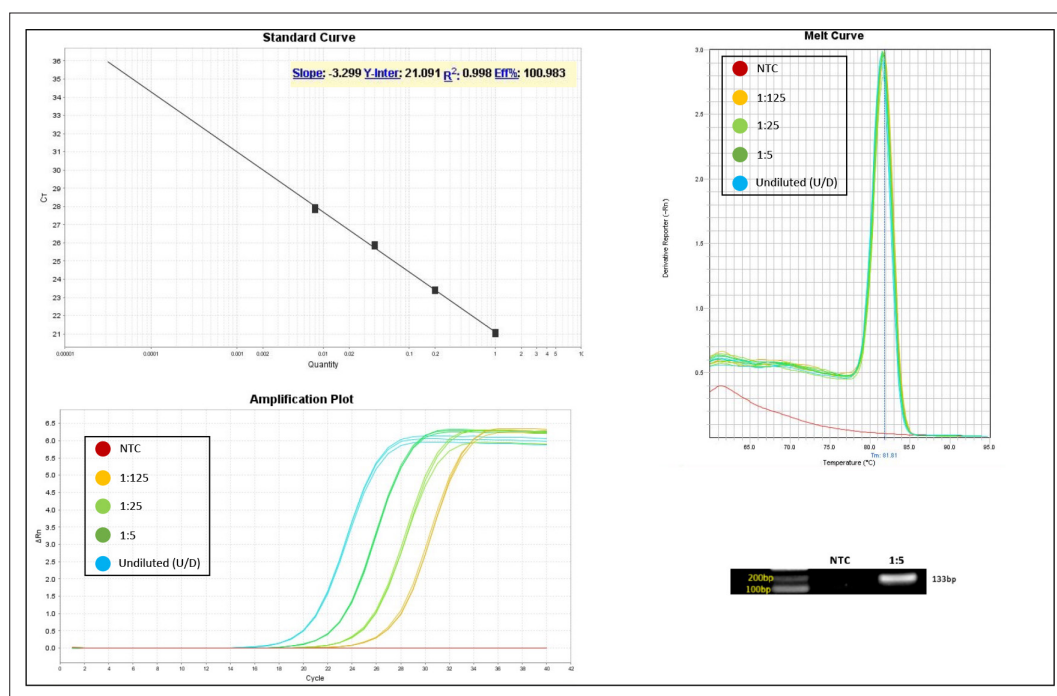
Appendix 1—figure 4. Validation of primer pairs used in RT-qPCR. Standard curve, melt curve, and amplification plot of amplification reactions of serial dilutions (1:5) are shown. Sample reactions were loaded on gel to validate amplicon size. NTC, non-template control.



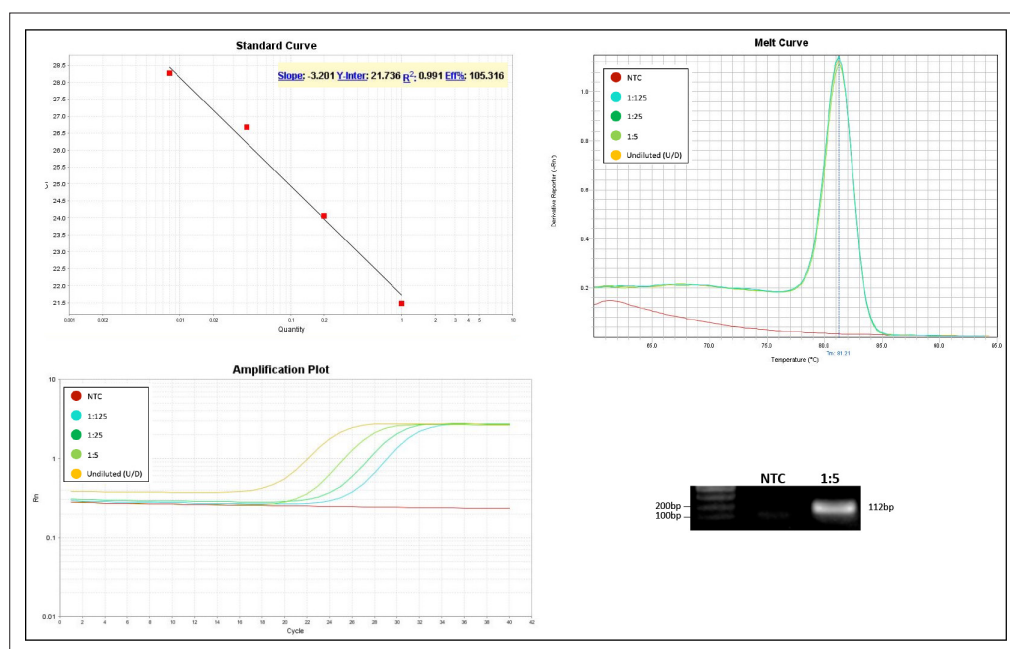
Appendix 1—figure 5. Validation of primer pairs used in RT-qPCR. Standard curve, melt curve, and amplification plot of amplification reactions of serial dilutions (1:5) are shown. Sample reactions were loaded on gel to validate amplicon size. The target was also amplified from RNA extracts of cells transfected with the pBI-mCherry construct as neg. control (mCh). NTC, non-template control.



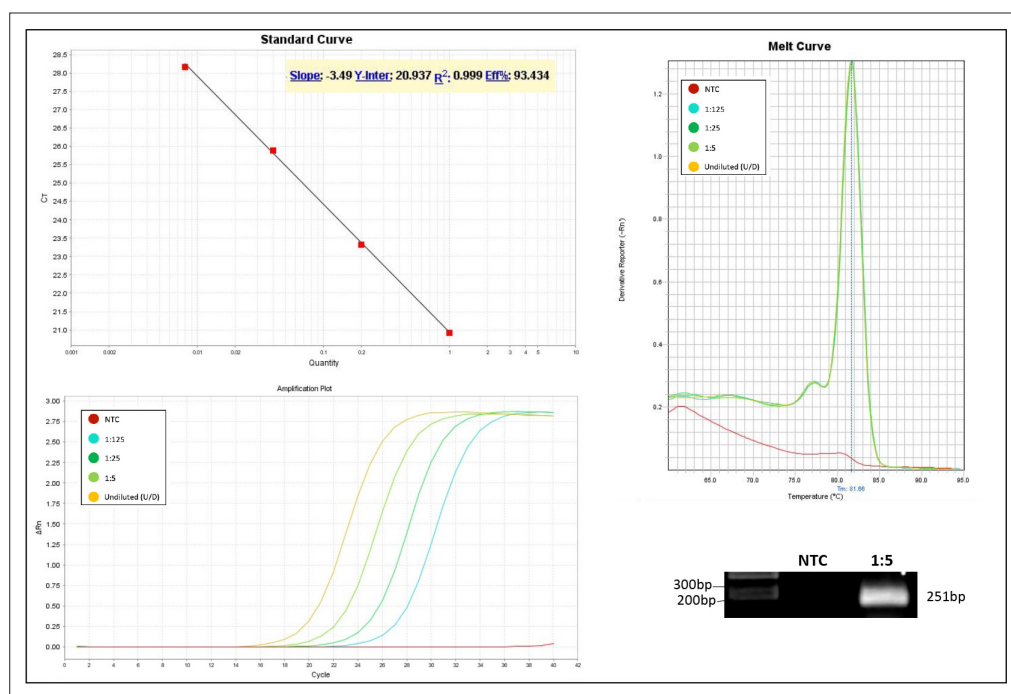
Appendix 1—figure 6. Validation of primer pairs used in RT-qPCR. Standard curve, melt curve, and amplification plot of amplification reactions of serial dilutions (1:5) are shown. NTC, non-template control.



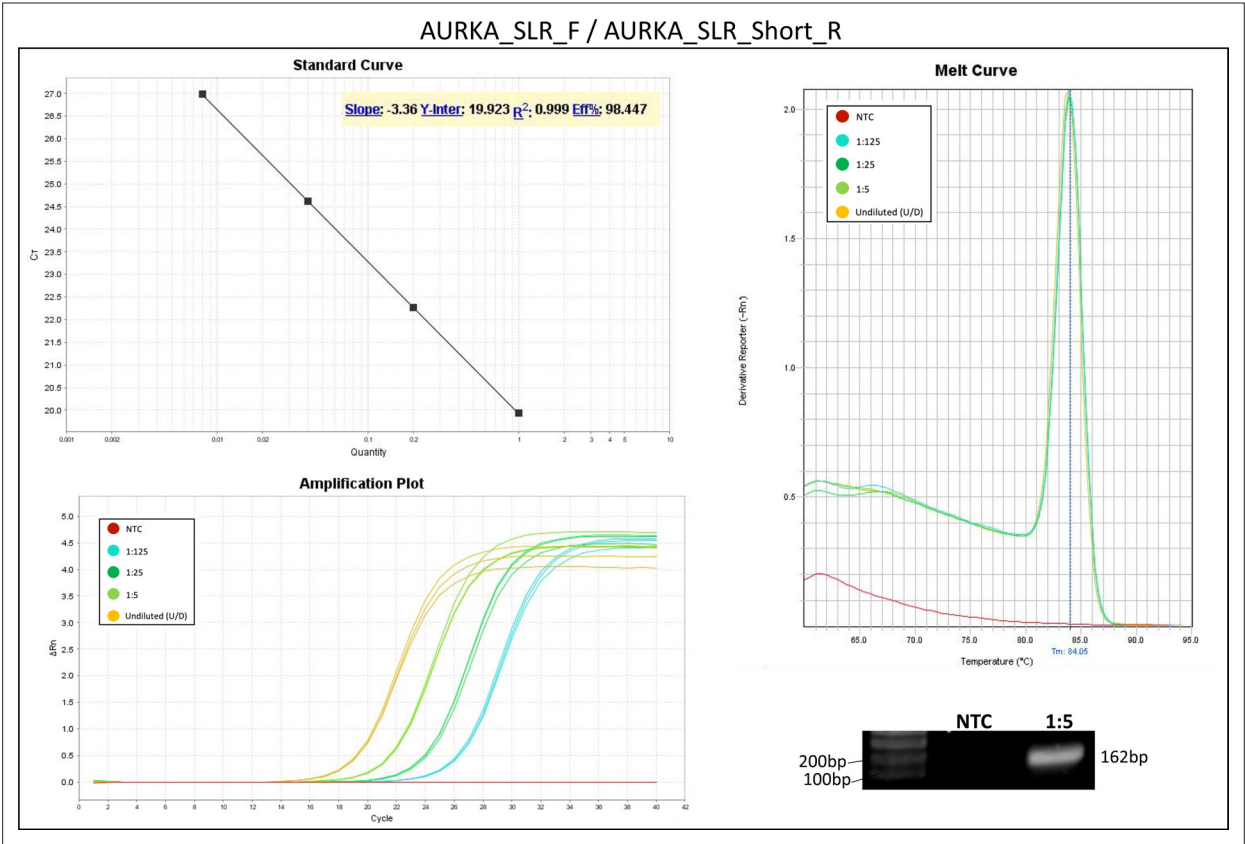
Appendix 1—figure 7. Validation of primer pairs used in RT-qPCR. Standard curve, melt curve, and amplification plot of amplification reactions of serial dilutions (1:5) are shown. Sample reactions were loaded on gel to validate amplicon size. NTC, non-template control.



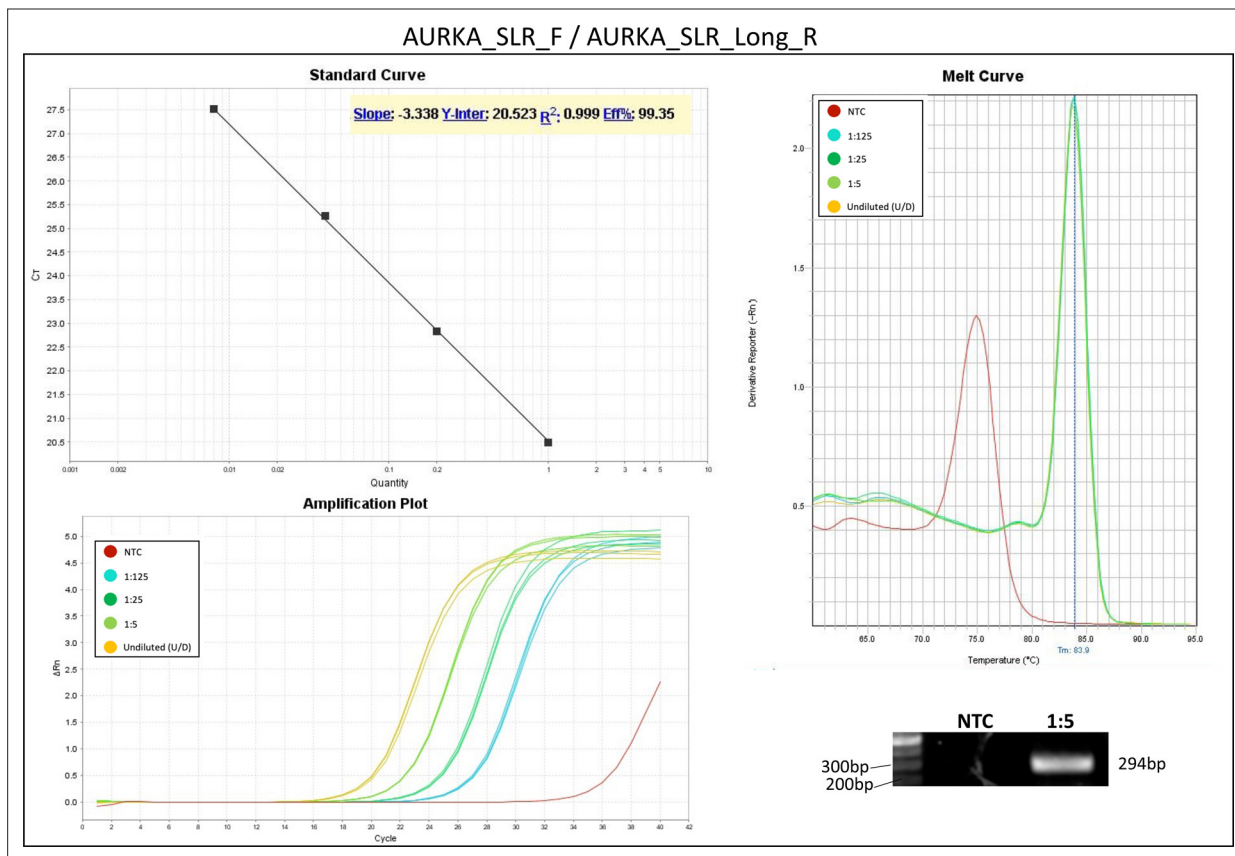
Appendix 1—figure 8. Validation of primer pairs used in RT-qPCR. Standard curve, melt curve, and amplification plot of amplification reactions of serial dilutions (1:5) are shown. Sample reactions were loaded on gel to validate amplicon size. NTC, non-template control.



Appendix 1—figure 9. Validation of primer pairs used in RT-qPCR. Standard curve, melt curve, and amplification plot of amplification reactions of serial dilutions (1:5) are shown. Sample reactions were loaded on gel to validate amplicon size. NTC, non-template control.



Appendix 1—figure 10. Validation of primer pairs used in RT-qPCR. Standard curve, melt curve, and amplification plot of amplification reactions of serial dilutions (1:5) are shown. Sample reactions were loaded on gel to validate amplicon size. NTC, non-template control.



Appendix 1—figure 11. Validation of primer pairs used in RT-qPCR. Standard curve, melt curve, and amplification plot of amplification reactions of serial dilutions (1:5) are shown. Sample reactions were loaded on gel to validate amplicon size. NTC, non-template control.